VIKAS GROUP OF INSTITUTIONS

(Sponsored by Mother Theresa Educational Society)
Approved by AICTE, New Delhi, PSI, New Delhi & Affiliated to JNTUK, Kakinada
ISO 9001 : 2015 Certified
Nunna – 521 212, Vijayawada Rural, NTR District, A.P. India.
Email: principal.9t@gmail.com

# 3.3.1 Number of research papers published per teacher in the Journals as notified on UGC CARE list during

## AY 2019

| S.No | Title of paper | Name of the author/s | Department of the teacher | Calendar Year of publication |
|---|---|---|---|---|
| 1 | Experiment Optimization of Mechanical Properities of AI7010/B4C/bn hybrid metal matrix Nanocomposites using Taguchi Technique | GOPICHAND DINISERAPU | Department of Mechanical Engineering | 2019 |
| 2 | Design sram emulation with precharge using error check bits | G.SEKHAR REDDY | Dept of ECE | 2019 |
| 3 | Design sram emulation with precharge using error check bits | S KISHORE BABU | Dept of ECE | 2019 |

PRINCIPAL/DIRECTOR
VIKAS GROUP OF INSTITUTIONS
NUNNA

IOP Publishing Mater. Res. Express 6 (2019) 105068 https://doi.org/10.1088/2053-1591/ab3bf8

Materials Research Express

RECEIVED
22 June 2019
REVISED
11 August 2019
ACCEPTED FOR PUBLICATION
16 August 2019
PUBLISHED
28 August 2019

PAPER

# Experimental optimization of mechanical properties of Al7010/$B_4C$/BN hybrid metal matrix nanocomposites using Taguchi technique

Gopichand Dirisenapu[1], Lingaraju Dumpala[2] and Pichi Reddy Seelam[3]

[1] Department of Mechanical Engineering, Jawaharlal Nehru Technological University, Kakinada, India; Department of Mechanical Engineering, Vikas group of institutions, Nunna, Vijayawada, India
[2] Department of Mechanical Engineering, Jawaharlal Nehru Technological University, Kakinada, India
[3] Department of Mechanical Engineering, Lakireddy Balireddy College of Engineering (A), Mylavaram, India

E-mail: dchanda310@gmail.com

Keywords: mechanical properties, Taguchi technique, ANOVA, $B_4C$, BN, ultrasonic assisted stir casting

## Abstract

The composite material properties largely dependent on the processing methods and the parameters employed during their manufacturing. In the present study, the effect of $B_4C$ and BN nanoparticles on tensile strength and microhardness of Al7010 hybrid metal matrix nanocomposite is investigated. The composite is prepared using ultrasonic assisted stir casting technique, and the effect of processing parameters like weight percentage of particles, stirrer speed, stirring time and temperature on ultimate tensile strength and microhardness are optimized using Analysis of Variance technique. The experiments are planned using Taguchi design of experiment based on the $L_{25}$ orthogonal array. In all the input parameters, the wt% of $B_4C$ and BN is most significant on ultimate tensile strength and microhardness followed by other parameters. Further, the verification of optimal experimental results the confirmation tests was conducted and also a percentage error is found.

## 1. Introduction

In modern days, the production of aluminium metal matrix composites (AMMCs) involves the addition of ceramic particles into aluminum and its alloys. The AMMCs exhibit many winsome mechanical properties like high stiffness, poor density, low ductility, poor fracture toughness, excellent strength and better corrosion resistance. The AMMCs are extensively used in marine, military, aerospace and automobile industries etc [1]. The aluminium metal matrix nanocomposites reinforced with ceramic nanoparticles into the aluminium matrix improve the ductility, fracture toughness and increased mechanical strength. The ceramic hard particles like $B_4C$, $TiB_2$, SiC, WC, $ZrB_2$, BN, etc., are used as reinforcements in AMMCs. Among these reinforcement particles, $B_4C$ particles possess outstanding bonding characteristics with aluminum and have low density (2.52 g $cm^{-3}$), excellent strength, good wear resistance and hardness, high melting point and is used as replacement for SiC and $Al_2O_3$ [2, 3].

The aluminium hybrid metal matrix nanocomposites (AHMMNCs) possess extraordinary mechanical properties such as high strength, poor density, low coefficient of thermal expansion, high ductility and toughness. It was formed by a combination of more than one different nano particle reinforced into the aluminum matrix to improve the toughness, ductility, decrease machining difficulties and improve wear resistance [4]. The nano boron carbide particles mixed with the aluminium matrix increases the mechanical strength and wear resistance of the composites (AMMNCs) and boron nitride nano particles is a potent reinforcement and acts as a solid lubricant and improves the toughness, wear resistance and acts as a self-lubricant in the AMMNCs [5]. Harichandran *et al* produced AHMMNCs with nano sized $B_4C$ and BN as reinforcement materials in the aluminium alloy using ultrasound assisted stir casting. The tensile strength of the composite is improved by 67% compared to the base alloy. The $B_4C$ nanocomposite addition with 6 wt% $B_4C$

particles gave better values of tensile and hardness compared to the other reinforced compositions. The wear resistance is better in hybrid combination with 4 wt% $B_4C$ and 2 wt% BN hybrid nanocomposite. In all combinations of hybrid composites, the impact energy and elongation are enhanced compared to nanocomposite [6]. Alihosseini *et al* fabricated the Al/$B_4C$ nanocomposites by high energy ball milling. Maximum Vickers hardness and compression strength is observed for 5 wt% $B_4C$ addition in Al nanocomposite [7]. The effect of $B_4C$ nano-sized particles reinforced in the aluminium metal matrix composites prepared by ball milling and hot press are studied by Sharifi *et al.* An increase in compressive strength, hardness and wear resistance with the increase in $B_4C$ particles is observed [8]. Chen *et al* investigated the microstructure and mechanical properties of Al 6061/$B_4C$ laminar composites produced by powder metallurgy—spark plasma sintering followed by extrusion and hot rolling. A uniform distribution of the $B_4C$ particles is observed in the composite. An increase in the yield strength, ultimate tensile strength and reduction in elongation is observed in rolled Al 6061/$B_4C$ laminar composites compared extruded Al 6061/$B_4C$ laminar composites [9].

Bhushan *et al* reported optimization of process parameters in Al 7075/10% SiC composite fabricated by stir casting technique. Taguchi technique is used to optimize the process parameters like holding temperature, holding time, stirring time and stirring speed on the performance parameter like porosity. The porosity of the composite increased with increase in stirring speed and decreased with the increase in holding time and temperature [10].

The effect of fly ash content in Al/fly ash composites produced by a stir casting technique on milling machine parameters optimized using Taguchi method is studied by Hayyawi *et al.* The results show that the mechanical properties improved with composite having 6 wt% fly ash [11]. Narender *et al* optimized the process parameters of Al 6061-red mud composite by means of the stir casting method using the Taguchi technique. The process parameters are weight percent of reinforcement, particle size and aging time with performance characteristics as impact strength. The aging time and particle size were found to be significant compared to the percentage of reinforcement particles [12].

The general fabrication methods for AMMNCs are stir casting [13], powder metallurgy [14], mechanical alloying, squeeze casting [15]. The nano sized ceramic particles $B_4C$ and BN is very difficult in getting uniform distribution and dispersion in the molten aluminium matrix by stir casting method because of low wettability and high surface to volume ratio of ceramic nanoparticles [6]. From the literature, it is found that, ultrasonic assisted stir casting technique helps in distribution and dispersion of nano sized ceramic particles uniformly and homogeneously in the molten aluminium matrix and improves the wettability and melt degassing between the aluminium matrix and reinforcement particles [16]. In this processes, the ultrasonic waves at 20 kHz frequency are introduced into the melt, which helps in uniform dispersion and distribution of the particles in the aluminum matrix. The acoustic cavitation produces the stress required to break the clustered and agglomerated nano ceramic particles and disperse them uniformly into the molten aluminium matrix [17].

However, the preparation of MMNCs using ultrasonic assisted stir casting with optimization of process parameters using Taguchi method is very limited. The Taguchi technique utilizes an orthogonal array for decreasing the number of experimental runs for optimizing considered parameters and their interactions. The aim of this research work is to produce aluminium hybrid metal matrix nanocomposites (AHMMNCs) with $B_4C$ and BN nanoparticles and optimize the process parameters of ultrasonic assisted stir casting. The process parameters are weight percentage of $B_4C$ and BN nanoparticles with 0.5, 1, 1.5, 2 and 2.5%, stirring speed 200, 300, 400, 500 and 600 RPM, stirring time 10, 15, 20, 25 and 30 min, processing temperature 700, 750, 800, 850 and 900 °C, with the performance characteristics as ultimate strength and microhardness. The effect of each control parameter on the ultimate strength and microhardness of the nanocomposites is evaluated using Analysis of variance (ANOVA).

## 2. Experimental details

### 2.1. Materials

In this study aluminium 7010 alloy is used as a matrix material. The Boron carbide and Boron nitride nanoparticles procured from Parashwamani metals, Mumbai-India is used as reinforcement particles. The SEM micrographs of $B_4C$ and BN nanoparticles are as shown in figures 1(a), (b) respectively. The properties of boron carbide and boron nitride are shown in table 1. The chemical composition of Al7010 alloy is represented in table 2.

The Ultrasonic assisted stir casting equipment used for preparation of composites is shown in figure 2. The setup consists of an electrical resistance heating furnace for melting the aluminium alloy, ultrasonic generator, ultrasonic probe, transducer, inert gas protection system. The required amount of aluminium alloy 7010 is melted inside the graphite crucible under inert gas protection and at 700, 750, 800 850 and 900 °C in the

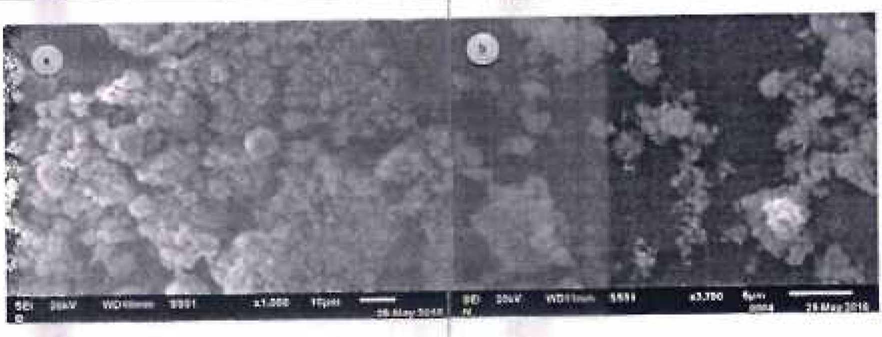


Figure 1. (a) SEM micrograph of $B_4C$. (b) SEM micrograph of BN.

Table 1. Properties of $B_4C$ and BN.

| Properties | $B_4C$ | BN |
|---|---|---|
| Particle size (nm) | 30–50 | 30–50 |
| Purity | 99.5 | 99.0 |
| Color | Black | White |
| Density (g $cm^{-3}$) | 2.52 | 2.28 |
| Elastic modulus (GPa) | 445 | 675 |
| Melting point (°C) | 2450 | 2973 |
| Thermal conductivity (W $mK^{-1}$) | 28 | 30 |

Table 2. Chemical composition of Al 7010 in wt%.

| Elements | Al | Zn | Mg | Cu | Fe | Zr | Si | Mn | Ti | Cr | Ni |
|---|---|---|---|---|---|---|---|---|---|---|---|
| wt% | Balance | 5.70–6.70 | 2.10–2.60 | 1.50–2.0 | 0.15 | 0.10–.016 | 0.12 | 0.10 | 0.0360 | 0.050 | 0.050 |

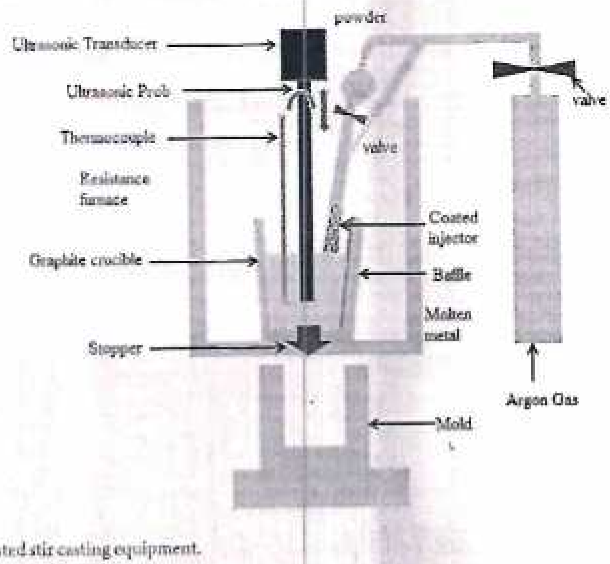


Figure 2. Ultrasonic assisted stir casting equipment.

electrical resistance heating furnace. The titanium probe with 20 mm diameter and 200 mm length is used to generate a frequency of 20 KHz with power of 20KW.

The BN, $B_4C$ particles are preheated to 450 °C and then mixed in equal proportions of 0.5, 1, 1.5, 2 and 2.5 wt% to aluminum alloy in the crucible. The melt is stirred with mechanical stirrer at a speed of 200, 300, 400, 500 and 600 RPM for 10, 15, 20, 25 and 30 min to create agitation. After that, the ultrasonic probe is immersed into

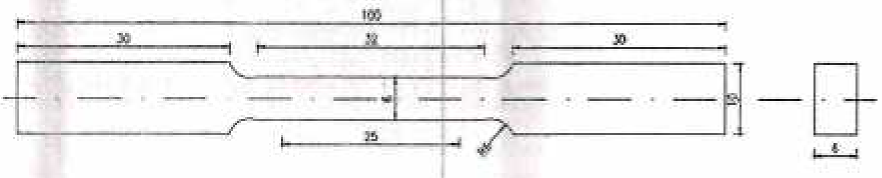


**Figure 3.** Tensile test specimen.

**Table 3.** Control parameters with their levels.

| | | | Control parameters and their levels | | | | |
|---|---|---|---|---|---|---|---|
| S No | Control parameters | Units | 1 | 2 | 3 | 4 | 5 |
| 1 | $B_4C$ and BN | wt% | 0.5 | 1 | 1.5 | 2 | 2.5 |
| 2 | Stirrer speed | RPM | 200 | 300 | 400 | 500 | 600 |
| 3 | Stirring time | Min | 10 | 15 | 20 | 25 | 30 |
| 4 | Processing temperature | °C | 700 | 750 | 800 | 850 | 900 |

the melt to a depth of 30 mm from the bottom of the crucible and vibrated for 30 min to break the clustered BN and $B_4C$ nanoparticles. The stopper is quickly removed from the bottom of the furnace and the melt is poured into the mild steel mould preheated at 600 °C. After cooling the specimen is removed from the mould. The standard test specimens are cut from the composites using the wire cut EDM machine for testing. The Ultimate tensile strength (UTS) of the composites is determined using the INSTRON-8801 testing machine. From the composite, the standard specimen is prepared according to ASTM E8-08 and the specimen drawing is shown in figure 3. The hardness of the specimen is measured using the Vickers hardness tester model DHB1. The test is conducted by applying load of 1000grams for the duration of 10 s. The average of three tested samples is reported.

The scanning electron microscope (SEM) model JEOL, JSM-660LV is used to determine the microstructures of the particles and the nanocomposites.

### 2.2. Optimization technique

The conventional experimental methods are lengthy, complex and difficult to execute. In this circumstance, on conducting more experiments, the process parameters and their levels also increase [18]. Therefore, Taguchi's method are best solutions for the design of experiments. It gives simple, effective and systematic approaches to optimize designs for performance, quality and cost [19]. In this paper, the statistical technique, i.e. Taguchi technique and ANOVA are used to achieve the optimum results. Optimized results for maximum values of ultimate strength and microhardness of Al 7010/$B_4C$/BN hybrid nanocomposites are determined.

### 2.3. Taguchi technique

Taguchi technique is one of the Design of experiment (DOE). This is a systematic and powerful tool and an effective methodology for optimization of process parameters which contains selections of parameters, experimental design, conducting experiments, data analysis and evaluating the optimum results and verification. This reduces the number of experimental runs compared to the other DOEs. In the present work, wt% of $B_4C$ and BN nanoparticles, stirring speed, stirring time, processing temperature are process parameters and the influence of each parameter on ultimate tensile strength and microhardness are evaluated. Taguchi method is invented for optimization of process and recognition of optimum levels of process parameters for the given responses. A Taguchi orthogonal array design offers an essay and effective way for reducing manufacturing cost and time, producing products with high quality. The selected control parameters and the orthogonal array are indicated in tables 3 and 4 respectively.

In taguchi method the quality characteristics are measured by transforming the experimental values of various responses into signal to noise (S/N) ratio. The S/N ratio characteristics are 'the higher, the better' and 'the lower, the better'. S/N ratios for 'higher the better' and 'lower the better' characteristics are calculated using equations (1) and (2) respectively,

$$\eta = -10\log_{10}\left[\frac{1}{n}\sum_{i=1}^{n}\frac{1}{y_i^2}\right] \quad (1)$$

Table 4. Design of experiment for $L_{25}$ orthogonal array.

| S No | $B_4C$ and BN(A) | Stirrer speed (B) | Stirring time(C) | Processing temperature(D) |
|---|---|---|---|---|
| 1 | 0.5 | 200 | 10 | 700 |
| 2 | 0.5 | 300 | 15 | 750 |
| 3 | 0.5 | 400 | 20 | 800 |
| 4 | 0.5 | 500 | 25 | 850 |
| 5 | 0.5 | 600 | 30 | 900 |
| 6 | 1 | 200 | 15 | 800 |
| 7 | 1 | 300 | 20 | 850 |
| 8 | 1 | 400 | 25 | 900 |
| 9 | 1 | 500 | 30 | 700 |
| 10 | 1 | 600 | 10 | 750 |
| 11 | 1.5 | 200 | 20 | 900 |
| 12 | 1.5 | 300 | 25 | 700 |
| 13 | 1.5 | 400 | 30 | 750 |
| 14 | 1.5 | 500 | 10 | 800 |
| 15 | 1.5 | 600 | 15 | 850 |
| 16 | 2 | 200 | 25 | 750 |
| 17 | 2 | 300 | 30 | 800 |
| 18 | 2 | 400 | 10 | 850 |
| 19 | 2 | 500 | 15 | 900 |
| 20 | 2 | 600 | 20 | 700 |
| 21 | 2.5 | 200 | 30 | 850 |
| 22 | 2.5 | 300 | 10 | 900 |
| 23 | 2.5 | 400 | 15 | 700 |
| 24 | 2.5 | 500 | 20 | 750 |
| 25 | 2.5 | 600 | 25 | 800 |

$$\eta = -10\log_{10}\left[\frac{1}{n}\sum_{i=1}^{n} y_i^2\right] \quad (2)$$

Where $\eta$ denotes S/N ratio of experimental values, $y_i$ represents the experimental value of the $i$th experiment and n is the total number of experiments. These characteristics are calculated in Minitab17.0® software. Table 5 shows the values of S/N ratio on every experiment in the $L_{25}$ orthogonal array for ultimate tensile strength and microhardness.

## 3. Result and discussion

### 3.1. Ultimate tensile strength (UTS)

The effects of control parameters on ultimate tensile strength (UTS) have been studied at five levels. Table 5 shows the results obtained from the experiments. The maximum and minimum UTS values of hybrid nanocomposite is 243 MPa and 204 MPa respectively.

The relative control parameters of these levels were 2 wt%, 500 RPM, 15 min, 900 °C and 0.5 wt%, 200 RPM, 10 min, 700 °C of $B_4C$ and BN, Stirrer speed, Stirring time and processing temperature respectively.

#### *3.1.1. Effect of control parameters on UTS*

The mean S/N ratio response values and ranks for UTS of composites at each level are tabulated in table 6. The deviation is calculated by the difference between the highest and lowest value of each parameter. It is observed that the weight percentage of particles are the most affecting parameter of all control parameters, followed by stirring time, stirrer speed and temperature.

The S/N ration plots shown in figure 4, describe that the UTS increased with increase in wt% of $B_4C$ and BN nanoparticles up to 2 thereafter decreases due to the finely dispersed reinforcement particles in the composite act as obstacles to the flow of materials and this increase the strength of the composite [8]. The increase in reinforcements beyond 2 wt% in the matrix, may form agglomerates or clusters resulting in decrease of the UTS in the composites.

The UTS is increased with the increase in stirrer speed up to 500 RPM and thereafter decreased because of the rise in stirring speed enhances the centrifugal current within the base melt and creates vortex, which in chance crumbles the $B_4C$ and BN clusters into particles distributed homogeneously. Further enhance in stirring



PRINCIPAL/DIRECTOR
VIKAS GROUP OF INSTITUTIONS
NUNNA - 521 212
Vijayawada Rural, NTR Dist., A.P.

**Table 5.** Experimental results with S/N ratios.

| S No | $B_4C$ and BN(A) | Stirrer speed (B) | Stirring time(C) | Processing temperature(D) | Ultimate tensile strength | S/N Ratio | Microhardness | S/N Ratio |
|---|---|---|---|---|---|---|---|---|
| 1 | 0.5 | 200 | 10 | 700 | 204 | 46.192 | 140.12 | 42.930 |
| 2 | 0.5 | 300 | 15 | 750 | 208 | 46.361 | 149.52 | 43.494 |
| 3 | 0.5 | 400 | 20 | 800 | 213 | 46.567 | 153.78 | 43.738 |
| 4 | 0.5 | 500 | 25 | 850 | 217 | 46.729 | 159.49 | 44.055 |
| 5 | 0.5 | 600 | 30 | 900 | 206 | 46.277 | 155.35 | 43.826 |
| 6 | 1 | 200 | 15 | 800 | 218 | 46.769 | 160.12 | 44.089 |
| 7 | 1 | 300 | 20 | 850 | 221 | 46.887 | 165.38 | 44.370 |
| 8 | 1 | 400 | 25 | 900 | 224 | 47.005 | 168.32 | 44.523 |
| 9 | 1 | 500 | 30 | 700 | 216 | 46.689 | 166.25 | 44.415 |
| 10 | 1 | 600 | 10 | 750 | 219 | 46.808 | 166.19 | 44.412 |
| 11 | 1.5 | 200 | 20 | 900 | 231 | 47.272 | 173.84 | 44.803 |
| 12 | 1.5 | 300 | 25 | 700 | 229 | 47.196 | 171.59 | 44.690 |
| 13 | 1.5 | 400 | 30 | 750 | 226 | 47.082 | 175.86 | 44.903 |
| 14 | 1.5 | 500 | 10 | 800 | 231 | 47.272 | 178.65 | 45.040 |
| 15 | 1.5 | 600 | 15 | 850 | 232 | 47.309 | 180.12 | 45.111 |
| 16 | 2 | 200 | 25 | 750 | 237 | 47.495 | 186.69 | 45.422 |
| 17 | 2 | 300 | 30 | 800 | 239 | 47.568 | 192.31 | 45.680 |
| 18 | 2 | 400 | 10 | 850 | 240 | 47.604 | 193.45 | 45.731 |
| 19 | 2 | 500 | 15 | 900 | 243 | 47.712 | 194.28 | 45.769 |
| 20 | 2 | 600 | 20 | 700 | 237 | 47.495 | 190.85 | 45.614 |
| 21 | 2.5 | 200 | 30 | 850 | 217 | 46.729 | 164.73 | 44.335 |
| 22 | 2.5 | 300 | 10 | 900 | 220 | 46.848 | 158.52 | 44.002 |
| 23 | 2.5 | 400 | 15 | 700 | 222 | 46.927 | 160.87 | 44.130 |
| 24 | 2.5 | 500 | 20 | 750 | 229 | 47.196 | 168.39 | 44.526 |
| 25 | 2.5 | 600 | 25 | 800 | 230 | 47.234 | 172.35 | 44.728 |

**Table 6.** Response table for ultimate tensile strength.

| Levels | $B_4C$ and BN (A) | Stirrer speed (B) | Stirring time (C) | Processing temperature (D) |
|---|---|---|---|---|
| 1 | 46.43 | 46.89 | 46.945 | 46.90 |
| 2 | 46.83 | 46.97 | 47.016 | 46.99 |
| 3 | 47.23 | 47.04 | 47.084 | 47.08 |
| 4 | 47.57 | 47.12 | 47.132 | 47.05 |
| 5 | 46.99 | 47.03 | 46.869 | 47.02 |
| Delta | 1.15 | 0.228 | 0.263 | 0.15 |
| Rank | 1 | 3 | 2 | 4 |

speed the UTS decreased due to deep vortex outcome in disorder and suction of air bubbles in the matrix melt increase in porosity and also at high stirrer speed the reinforcement is not properly mixed with the matrix material because of the high velocity to form vortex in the semi-solid state slurry [20]. This may be the reason for decrease in UTS beyond 500 RPM [21]. The formation of vortex in the matrix melt, sucks the particles into liquid due to the pressure difference between the inner and outer surface of melt. The UTS raised to increase in stirring time up to 25 min and there after decrased due to the centrifugal currents within the molten base metal collapse the clusters and disperse the particles from particles free provinces to throughout the base metal. Furthur enhance in stirring time the UTS reduced because of longer, stirring time creates extra agitation in the molten metal matrix which enhances the tendency to form porosity [20]. The UTS enhances as processing temperature increases up to 800 °C due to enhance in processing temperature, reduce the viscosity the lower in viscosity increases the easiness of stirring and enhances the centrifugal currents in the molten base metal. The clusters are dispersed and homogeneously distributed in the melt. The low porosity of the casting was prepared due to cooling rate at 800 °C is best which allows the necessary time to reduce the absorbed gases. Further, increase in processing temperature the UTS was reduced because of rise in processing temperature 800 °C to 900 °C decreases the viscosity of the aluminium melt. The particles were moving quickly and rapid and easily within the aluminium melt due to particles achieve high energy at elevated temperatures. The cooling rate at 900 °C is

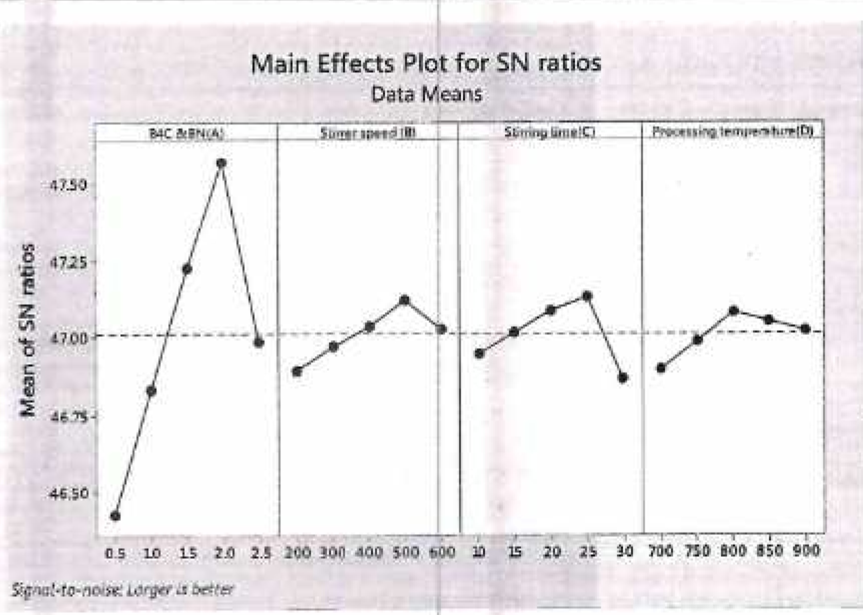


**Figure 4.** Control parameters effect on ultimate tensile strength

**Table 7.** ANOVA results for ultimate tensile strength.

| Source | DoF | Seq SS | Adj SS | Adj MS | F | P | %Cont |
|---|---|---|---|---|---|---|---|
| $B_4C$ and BN (A) | 4 | 3.70 | 3.70 | 0.92 | 155.07 | 0.000 | 87.87 |
| Stirrer speed (B) | 4 | 0.14 | 0.14 | 0.036 | 5.97 | 0.016 | 3.38 |
| Stirring time (C) | 4 | 0.22 | 0.22 | 0.056 | 9.31 | 0.0042 | 5.28 |
| Processing temperature (D) | 4 | 0.098 | 0.098 | 0.025 | 4.13 | 0.042 | 2.34 |
| Residuals error | 8 | 0.048 | | | | | 1.13 |
| Total | | 4.21 | | | | | 100 |

slower compared with other processing temperatures due to the porosity of the casting is increased [20]. The optimum condition for the UTS is given by control parameter $A_4B_4C_4D_3$.

#### 3.1.2. *Analysis of variance (ANOVA)*

The ANOVA technique is used for determining the effect of individual control parameters on the performance characteristic parameters. The ANOVA analysis is carried out based on the P-value for each independent control parameter. So the parameters with P-value less than 0.05 is considered as statistically significant, the P-value greater than 0.05 the parameters is considered as insignificant, that means no effect is done in the process.

Table 7 shows the ANOVA results, it was observed that the wt% of $B_4C$ and BN (87.87), stirrer speed (3.38), Stirring time (5.28) and processing temperature (2.34) and the P-value of all four control parameters is less than 0.05, this means that the control parameters are significantly affecting the UTS. In this weigh percentage of reinforcement is the most influencing parameter followed by other control parameters.

The normal probability plots of residuals gained from ANOVA of composites is shown in figure 5. It is reported that, all the residuals are aligned near to the fitted distribution line indicating the perfect fitness of selected distribution.

Figure 6 shows the plot of residual verses fitted values for UTS. The residuals scattered randomly about the zero line, which entails that the residuals have a constant variance.

### 3.2. Microhardness

Table 5 shows the experimental microhardness values. The maximum and minimum microhardness values of hybrid nanocomposites are 194.28 and 140.12 respectively.

The relative control parameters for that level are 2 wt%, 500 RPM, 15 min, 900 °C and 0.5 wt%, 200 RPM, 10 min, 700 °C of $B_4C$ and BN, stirrer speed, stirring time and processing temperature respectively.

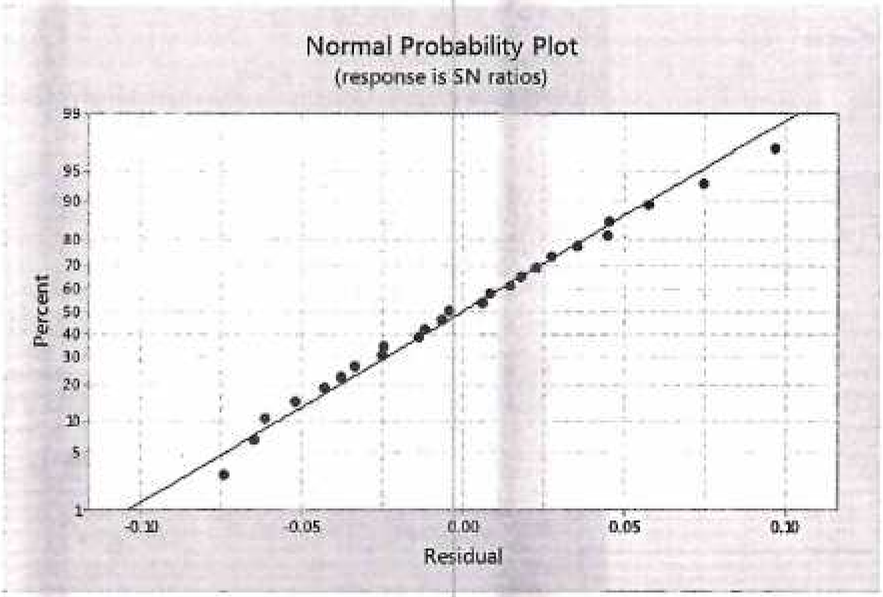


**Figure 5.** Normal probability plot of S/N ratio for UTS.

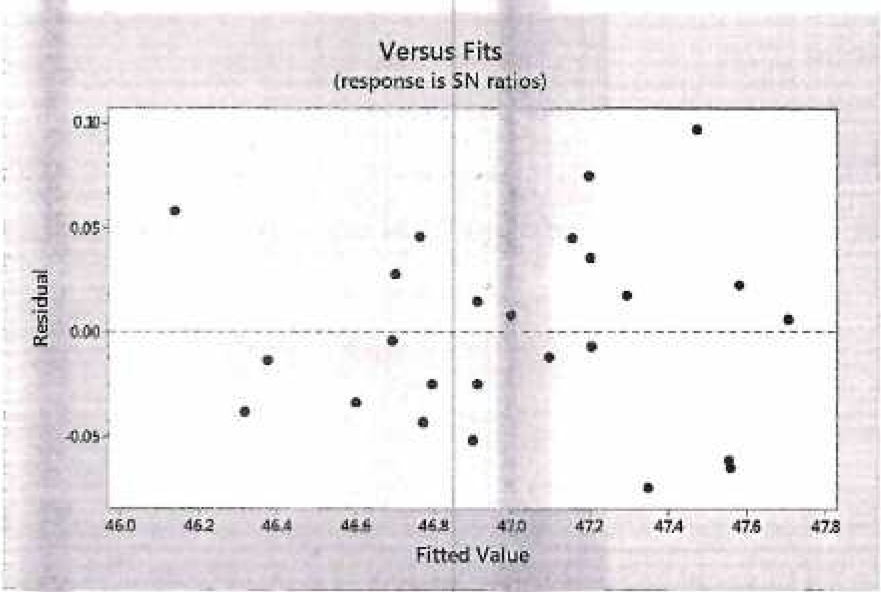


**Figure 6.** Plot for residual verses fitted value of S/N ratio for UTS.

*3.2.1. Effect of control parameters on Microhardness*

Table 8 shows the mean S/N ratio values for microhardness of the composite at each level. The data values are evaluated by the difference between the highest and lowest value of each parameter. It is reported that most affected parameter is wt% of $B_4C$ and BN, followed by the stirring time, stirrer speed and process temperature.

The main response plot of the S/N ratio shown in figure 7, depicts that microhardness increased with increase in wt% of $B_4C$ and BN nanoparticles up to 2 thereafter decreases [22]. The initial increase in microhardness of the nanocomposites due to their uniform distribution of the reinforcement particles is in the matrix which acts as obstacles to the flow of material. With further increase of particles, clusters may be formed in the matrix and results in the decrease of the microhardness. The microhardness increased with the increase of stirrer speed up to 500 RPM, then after with increase in speed the microhardness decreased due to the rise in

Table 8. Response table for microhardness.

| Levels | $B_4C$ and BN (A) | Stirrer speed (B) | Stirring time (C) | Processing temperature (D) |
|---|---|---|---|---|
| 1 | 43.61 | 44.32 | 44.423 | 44.36 |
| 2 | 44.36 | 44.45 | 44.518 | 44.55 |
| 3 | 44.91 | 44.60 | 44.610 | 44.66 |
| 4 | 45.64 | 44.76 | 44.684 | 44.72 |
| 5 | 44.34 | 44.74 | 44.632 | 44.58 |
| Delta | 2.03 | 0.445 | 0.052 | 0.36 |
| Rank | 1 | 2 | 4 | 3 |

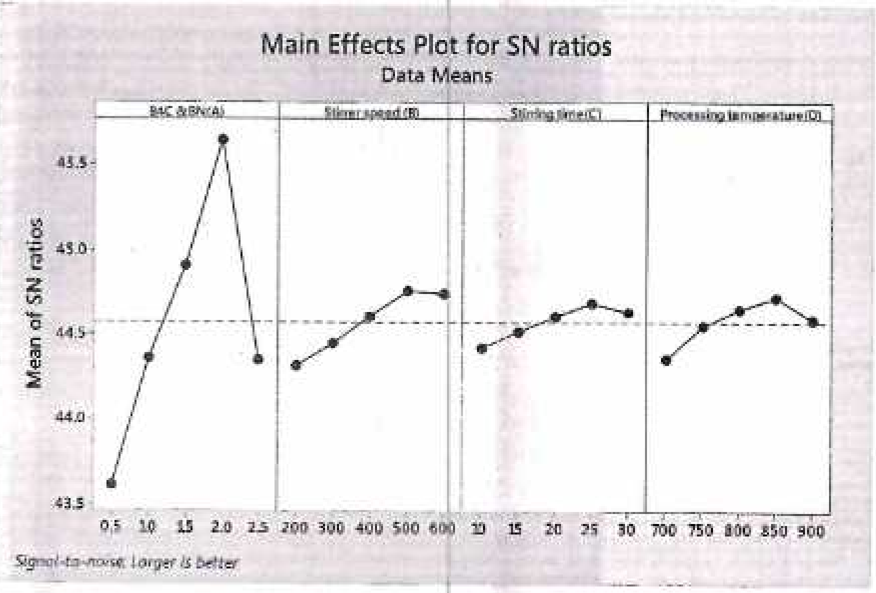


Figure 7. Control parameters effect on microhardness.

stirring speed enhances the centrifugal current within the base melt and creates vortex, which in chance crumbles the $B_4C$ and BN clusters into particles distributed homogeneously.

With the increase of stirring time the microhardness increased upto 25 min, and thereafter decreased because of the centrifugal currents within the molten base metal collapse the clusters and disperse the particles from particles free provinces to throughout the base metal. The microhardness increases with increase in processing temperature up to 850 °C, then after decreased, because of the enhance in processing temperature, reduce the viscosity the lower in viscosity increases the easiness of stirring and enhances the centrifugal currents in the molten base metal. The clusters are dispersed and homogeneously distributed in the melt and also high temperature does not restrict the vortex of molten metal to form clusters. Therefore, from the analysis the optimum combination of control parameters for microhardness is $A_4B_4C_4D_4$.

*3.2.2. Analysis of variance (ANOVA)*

The effect of control parameters individually on the response output parameters is evaluated using ANOVA technique. The ANOVA method is performed based on the F-value and P-value, taking significant effect of contribution of input parameters on the response parameter at a level of significance of 0.05, i.e., the P-value is greater than 0.05 the parameters are insignificant. The P-value less than 0.05 the parameters are significant.

The ANOVA results are shown in table 9. It indicates that, percentage of contributions of control parameters were wt% of $B_4C$ and BN with 89.23, stirrer speed with 5.68, stirring time with 1.66, processing temperature with 2.97 respectively. The wt% of $B_4C$ and BN parameter is most influencing parameter on the microhardness followed by others.

Figure 8 shows the normal plots of residuals. It indicates that all the residuals are very close to the inclined line, which verifies normal probability distribution of ANOVA.

Table 9. ANOVA results for Microhardness.

| Source | DoF | Seq SS | Adj SS | Adj MS | F | P | %Cont |
|---|---|---|---|---|---|---|---|
| $B_4C$ and BN (A) | 4 | 11.428 | 11.428 | 2.857 | 407.432 | 0.0000 | 89.23 |
| Stirrer speed (B) | 4 | 0.7281 | 0.7281 | 0.182 | 25.957 | 0.000 12 | 5.68 |
| Stirring time (C) | 4 | 0.2127 | 0.2127 | 0.053 | 7.5860 | 0.007 89 | 1.66 |
| Processing temperature (D) | 4 | 0.3814 | 0.3814 | 0.0953 | 13.599 | 0.0012 | 2.97 |
| Residuals error | 8 | 0.0561 | | | | | 0.43 |
| Total | | 12.807 | | | | Total | 100 |

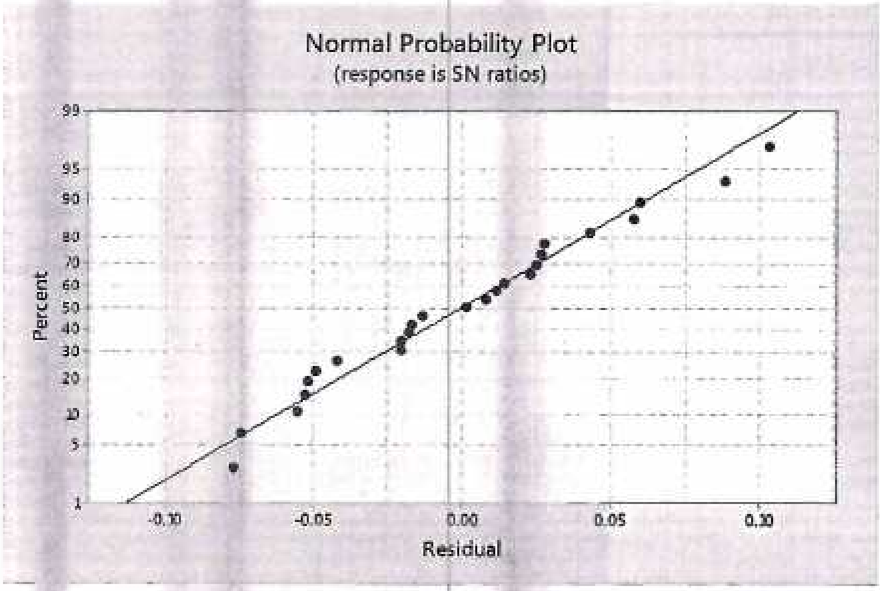


Figure 8. Normal probability plot of S/N ratio for microhardness.

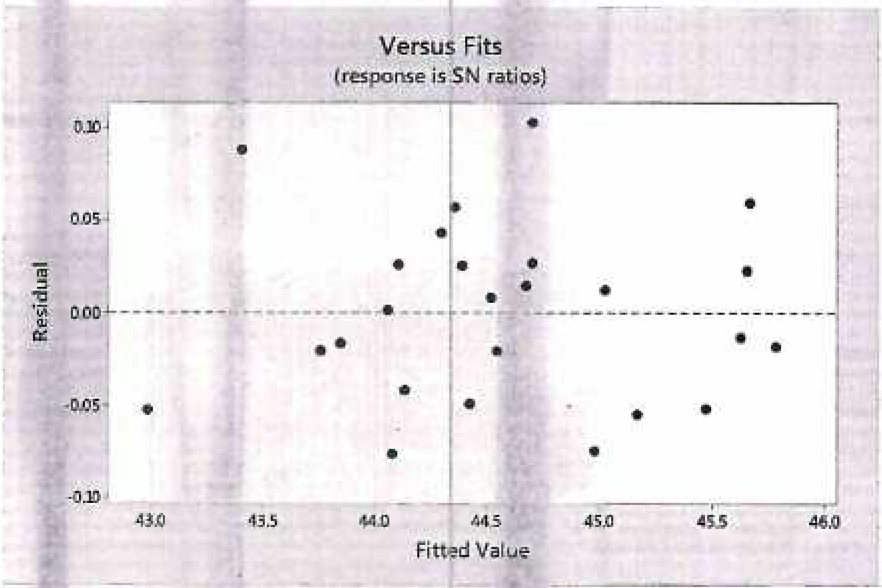


Figure 9. Plot for Residual verses Fitted value of S/N ratio for microhardness.

Table 10. Conformation test results.

| S no. | Optimum condition | Predicted value | Experimental value | % of error |
|---|---|---|---|---|
| 1 | $A_4B_4C_4D_3$ | 243 | 245 | 0.81 |
| 2 | $A_4B_4C_4D_4$ | 194.24 | 196.38 | 1.08 |

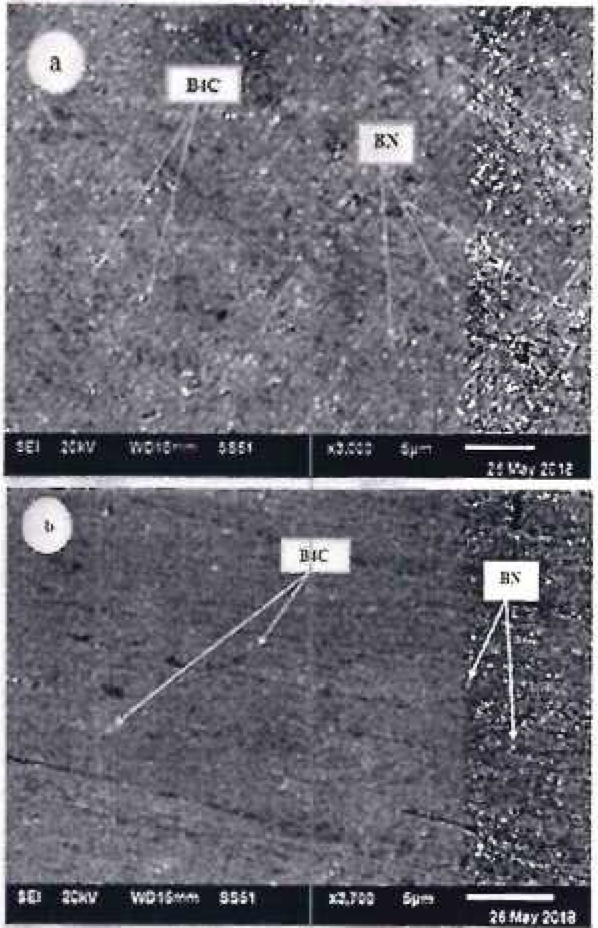


Figure 10. (a) SEM microstructure of Al7010/$B_4C$/BN nanocomposites of Ultimate tensile strength at 2 wt% of $B_4C$ and BN, Stirrer Speed of 500 RPM, Stirring time of 25 min and Processing temperature of 800 °C. (b) SEM microstructure of Al7010/$B_4C$/BN nanocomposites of Microhardness at 2 wt% of $B_4C$ and BN, Stirrer Speed of 500 RPM, Stirring time of 25 min and Processing temperature of 850 °C.

The residual verses fitted values for microhardness is plotted in figure 9. It is observed that residuals are scattering randomly about the zero line. So that the model having constant variance with errors are negligible.

### 3.2.3. Confirmation experiment

The confirmation experiments were conducted for the optimum control parametric condition by Taguchi method. It is the final step to observe the predicted and validation improvements are based on the optimal control parameters. The optimum combination level of control parameters are $A_4B_4C_4D_3$ and $A_4B_4C_4D_4$ for UTS and Microhardness respectively. Table 10 indicated the comparison of average values gained from conformation tests with the experimental and predicted results. The figures 10(a), (b) shows the SEM images for optimum condition of the composite. It was seen that the particles are dispersed and distributed evenly throughout the base matrix is observed because of sufficient factors were incorporated for preparing the composites. Figure 11 shows that the elemental maps of Al7010/$B_4C$/BN nanocomposite of figure 10. It represented the existence and distribution of aluminum (figure 11(a)), boron (figure 11(b)), carbon

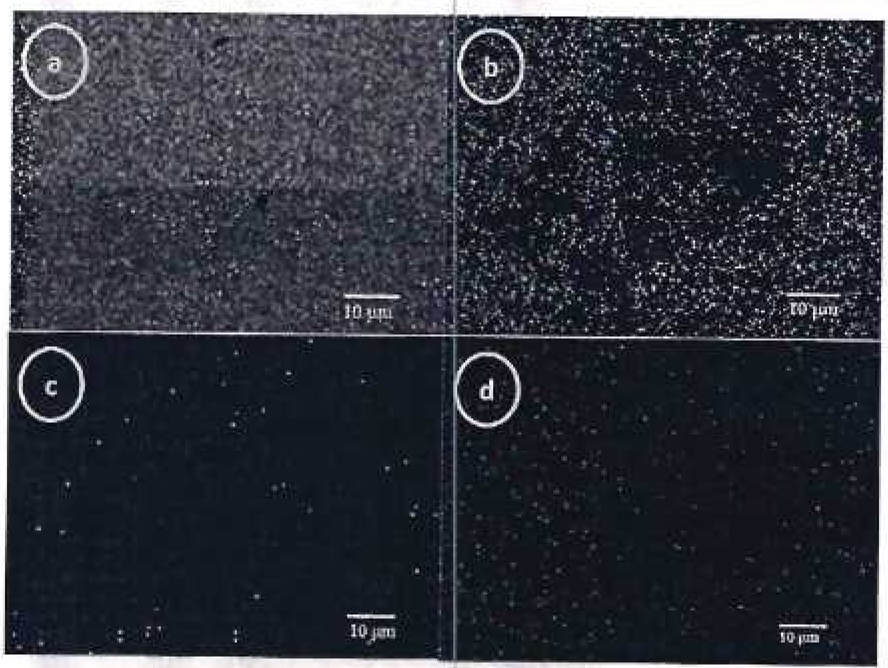


**Figure 11.** EDX elemental map analysis of the Al7010/$B_4C$/BN nanocomposite (a) Al (aluminium), (b) B (Boron), (c) C (Carbon) and (d) N (Nitrogen).

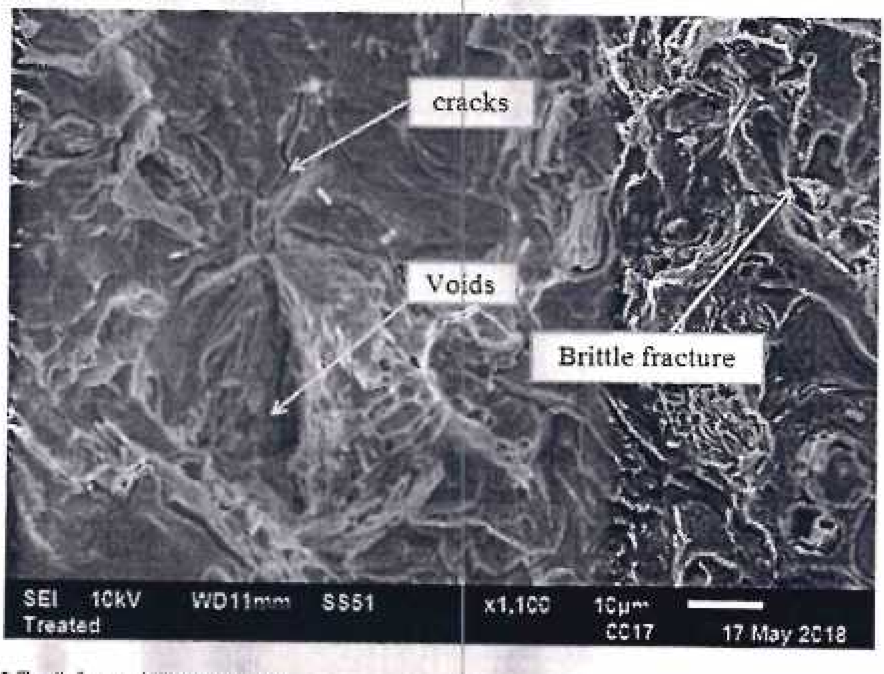


**Figure 12.** Tensile fractured SEM micrograph.

(figure 11(c)) and nitrogen (figure 11(d)), as shown by the electron map. The SEM of the fractured tensile test specimens is shown in figure 12, it was observed that the composite is described by voids, ridges and cracks because of ductile, elastic and brittle nature of the composites due to which the tensile strength increases.



PRINCIPAL/DIRECTOR
VIKAS GROUP OF INSTITUTIONS
NUNNA - 521 212
Vijayawada Rural, NTR Dist., A.P.

## 4. Conclusion

The following conclusions are drawn from the experimental investigation, which is based on the optimization of ultrasonic assisted stir casting process parameters on the mechanical properties of hybrid metal matrix nanocomposites.

- The optimum design parameter condition for maximum ultimate tensile strength is obtained from Taguchi $L_{25}$ orthogonal array is $A_4B_4C_4D_3$.
- The maximum microhardness value is gained by optimum condition $A_4B_4C_4D_4$ from Taguchi orthogonal array $L_{25}$.
- The ANOVA results revealed that wt% of $B_4C$ and BN (87.87) has the strongest effect on UTS, followed by other control parameters such as stirrer speed (3.38), stirring time (5.28) and processing temperature (2.34).
- The percentage of contribution of process parameters are wt% of $B_4C$ and BN of 89.23, stirrer speed of 5.68, stirring time of 1.66 and processing temperature of 2.97, which are described from the ANOVA results. However, the most influencing control factor on microhardness is wt% of $B_4C$ and BN.
- The evaluated optimum combinations of ultrasonic assisted stir caring process parameters of Al7010/$B_4C$/BN nanocomposite were fulfilled the existential necessity, which is based on the confirmation test.
- The SEM microstructure and EDX elemental maps of optimum condition of hybrid nanocomposite showed that the nanoparticles are evenly distributed in aluminium matrix. The analysis of fractured images of the tensile specimen was observed that the failure occurs due to ductile, elastic and brittle nature of the composite.

## ORCID iDs

Gopichand Dirisenapu https://orcid.org/0000-0002-3533-6925

## References


[1] Kaushik N and Singhal S 2018 Hybrid combination of Taguchi-GRA-PCA for optimization of wear behavior in AA6063/SiCp matrix composite *Production & Manufacturing Research* 6 171–189

[2] Toptan F, Kilicarslan A, Karaaslan A, Cigdem M and Kerti I 2010 Processing and microstructural characterisation of AA 1070 and AA 6063 matrix $B_4$Cp reinforced composites *Mater. Des.* 31 S87–S91

[3] Baradeswaran A E P A and Elaya Perumal A 2013 Influence of $B_4C$ on the tribological and mechanical properties of Al 7075–$B_4C$ composites *Composites Part B: Engineering* 54 146–152

[4] Kannan C and Ramanujam R 2017 Comparative study on the mechanical and microstructural characterization of AA 7075 nano and hybrid nanocomposites produced by stir and squeeze casting *J. Adv. Res.* 8 309–319

[5] Selvam J D R, Dinaharan I, Vibin Philip S and Mashinini P M 2018 Microstructure and mechanical characterization of *in situ* synthesized AA6061/($TiB_2$ + $Al_2O_3$) hybrid aluminum matrix composites *J. Alloys Compd.* 740 529–535

[6] Harichandran R and Selvakumar N 2018 Microstructure and mechanical characterization of ($B_4C$ + h-BN)/Al hybrid nanocomposites processed by ultrasound assisted casting, *International Journal of Mechanical Science* 144 814–826

[7] Alihosseini H and Dehghani K 2017 Microstructure characterization, mechanical properties, compressibility and sintering behavior of Al-$B_4C$ nanocomposite powders *Adv. Powder Technol.* 28 2126–2134

[8] Sharifi E M, Karimzadeh F and Enayati M H 2011 Fabrication and evaluation of mechanical and tribological properties of boron carbide reinforced aluminum matrix nanocomposites *Mater. Des.* 32 3263–3271

[9] Chen H-S, Wang W-X, Nie H-H, Zhou J, Li Y-L and Zhang P 2017 Microstructure and mechanical properties of $B_4C$/6061Al laminar composites fabricated by power metallurgy *Vacuum* 143 365–370

[10] Bhushan R K, Kumar S and Das S 2009 Optimisation of porosity of 7075 Al alloy 10% SiC composite produced by stir casting process through Taguchi method *International Journal of Materials Engineering Innovation* 1

[11] Rabeea H A, Al-Ethari H and Haleem A H 2016 Investigation of mechanical and machining properties of recycled al-fly ash composites *Advances in Natural and Applied Sciences* 10 50–60

[12] Panwar N and Chauhan A 2018 Optimizing the effect of reinforcement, particle size and aging on impact strength for Al 6061-red mud composite using Taguchi technique *Sādhanā* 44 101

[13] Kumar R A, Sait A N and Subramanian K 2018 Evaluation of wear behaviour for Al/$B_4C$/fly ash composites by stir casting process *Journal of Scientific & industrial Research* 77 282–287

[14] Reddy S P, Ramana B and Chennakesava Reddy A 2013 Sintering characteristics of Al-Pb/fly-ash metal matrix composites *Trans. Indian Inst. Met.* 66 87–95

[15] Maj J, Basista M, Węglewski W, Bochenek K, Strojny-Nędza A, Naplocha K, Panzner T, Tatarková M and Fiori F 2018 Effect of microstructure on mechanical properties and residual stresses in interpenetrating aluminum-alumina composites fabricated by squeeze casting *Materials Science and Engineering: A* 715 154–162

[16] Poovazhagan L, Kalaichelvan K and Rajadurai A 2014 Preparation of SiC nano-particulates reinforced aluminum matrix nanocomposites by high intensity ultrasonic cavitation process *Trans. Indian Inst. Met.* 67 229–237

[17] Pasumarthi P, Absar S and Choi H 2016 The effect of geometrical parameters on the characteristics of ultrasonic processing for metal matrix nanocomposites (MMNCs) *J. Manuf. Processes* 24 382–390
[18] Kong X, Yang L, Zhang H, Chi G and Wang Y 2017 Optimization of surface roughness in laser-assisted machining of metal matrix composites using Taguchi method *The International Journal of Advanced Manufacturing Technology* 89 529–542
[19] Reddy S P, Chandrasekhara Rao P V and Kolli M 2018 Effect of reinforcement on compacting characteristics of aluminum/10-$Al_2O_3$/fly ash metal matrix composite *J. Test. Eval.* 48
[20] Moses J J, Dinaharan I and Joseph Sekhar S 2016 Prediction of influence of process parameters on tensile strength of AA6061/TiC aluminum matrix composites produced using stir casting *Transactions of Nonferrous Metals Society of China* 26 1498–1511
[21] Ruirui W, Zheng Y and Qiushu L 2017 Microstructure and mechanical properties of 7075 Al alloy based composites with $Al_2O_3$ nanoparticles *Int. J. Cast Met. Res.* 30 337–340
[22] Singh G and Goyal S 2018 Microstructure and mechanical behavior of AA6082-T6/SiC/$B_4C$-based aluminum hybrid composites *Part. Sci. Technol.* 36 154–161

# DESIGN SRAM EMULATION WITH PRECHARGE USING ERROR CHECK BITS

[1]BATTA APARNA, [2]G. SEKHAR REDDY, [3] S KISHORE BABU
[1]M.Tech scholar, Dept of ECE, Vikas group of institutions, Nunna, Vijayawada, A.P
[2]Assistant Professor, Dept of ECE, Vikas group of institutions, Nunna, Vijayawada, A.P
[3]HOD & Associate Professor, Dept of ECE, Vikas group of institutions, Nunna, Vijayawada, A.P

**ABSTRACT: Modern ICs are enormously complicated due to decrease in device size. For high-speed memory applications such as cache, a SRAM is often used. In this paper SRAM is designed with pre charge bits using error check bits. The memories can be protected with check bits to detect errors. Single-bit errors corrected when memories are protected with check bit. by employing the gated pull down path and boosting scheme, search speed will be increased. By considering the number of mismatch and discharging speed, the discharging is adaptively controlled in the proposed system. At last the proposed system gives effective results in terms of speed and delay.**

**KEY WORDS: SRAM (static random access memory), pre charge unit, check bits, content addressable memory, error correction and location schemes.**

## I.INTRODUCTION

As CMOS innovation downsizes to nano scale and recollections are joined with an expanding number of electronic frameworks, the delicate mistake rate in memory cells is quickly expanding, particularly when recollections work in space conditions due to ionizing impacts of barometrical neutron, alpha-molecule, and enormous beams. Albeit single piece upset is a noteworthy worry about memory unwavering quality, multiple cell upsets have turned into a genuine dependability worry in some memory applications. So as to make memory cells as issue tolerant as could reasonably be expected, some error correction codes (ECCs) have been generally used to secure recollections against delicate mistakes for quite a long time. For instance, the punctured different set codes have been utilized to manage MCUs in Recollections. Yet, these codes require more area, power, and delay overheads. Since the encoding and unraveling circuits are increasingly in these confounded codes [1-2].

The general thought for accomplishing blunder location and adjustment is to include some excess (i.e., some additional information) to a message, which recipient can use to check consistency of the conveyed message, and to get information resolved to be degenerate. Mistake identification and redress plan can be either methodical or non-efficient. In a deliberate plan, the transmitter sends the interesting information, and connects a fixed number of check bits (or equality information), which are gotten from the information bits by some deterministic calculation. On the off chance that just the mistake discovery is required, a recipient would simple be able to apply a similar calculation to the got information bits and contrast its yield and the get check bits; if the qualities don't coordinate, a blunder has happened sooner or later all through the transmission [3].

Error correcting codes are normally utilized in lower-layer correspondence, As well with respect to solid stockpiling in media, for example, CDs, DVDs, hard plates and RAM. Static RAM based Field-Programmable Gate Arrays (FPGAs) are most broadly utilized in assortment of utilizations chiefly because of brief time-to market time, adaptability, high thickness, and cost-proficiency. SRAM-based FPGA stores rationale cells arrangement information in the static memory composed as a variety of locks. FPGA is utilized for planning complex computerized circuits. Power utilization is likewise diminished by utilizing SRAM [4]. The power utilization of SRAM differs generally relying upon how much of the time it is gotten to; it very well may be as eager for power as unique RAM, when utilized at high frequencies, and a few ICs can devour numerous watts at full data transmission. Then again, static RAM utilized at a to some degree slower pace, for example, in applications with Moderately timed microchips, draws next to no power and can have an almost unimportant power utilization when sitting inert – in the area of a couple of miniaturized scale watts.

A few procedures have been executed to oversee control utilization of SRAM-based memory structures. FPGA gadget adjustable by SRAM comprises of a variety of programmable rationale squares interconnected by a programmable steering system and I/O squares. SRAM-based FPGA gadgets are getting to be famous in view of their elite, diminished advancement cost and re programmability. FPGAs dependent on a nanometer innovation with denser incorporation plans. Recollections are a standout amongst the most broadly utilized components in electronic frameworks. Radiation in the earth genuinely influences the usefulness of a circuit [5].

A single event upset (SEU) happens when a charged molecule, present in the earth, hits the silicon of a circuit presenting a mistake in the framework. Such mistakes in FPGA gadget influences the usefulness of the mapped plan likewise called as Soft blunders. A soft error won't harm a framework's equipment, the main harm is to the information that is being handled in the memory. To address this issue, Built-in Current Sensors (BICS) have as of late been connected related to Single Error Correction/Double Error Detection (SEC-DED) codes to shield recollections from MBUs. In any case, by utilizing those strategies no one but SEU could be revised. For both the recognition and revision of mistakes, a nonexclusive scouring plan to recreate the incorrect arrangement outline dependent on the idea of Erasure coding calculation is presented in this paper. In this sort of Erasure coding calculation, MBUs are identified by utilizing the interleaving separation which is additionally grouped into flat and vertical equality [6].

The outcomes got have demonstrated that this methodology have a lower defer overhead over different codes. built in current sensors (BICS) are actualized to help with single-blunder rectification and twofold mistake identification codes to give insurance against MBUs. Nonetheless, this strategy can just address two mistakes in a word .In this paper, the design of SRAM using error check bits is proposed. The actualized network code use calculation (number expansion and whole number subtraction) to identify blunders. Plus, the deletion codes is actualized to limit the zone overhead of additional circuits (encoder and decoder) without exasperating the entire encoding and disentangling forms.

## II. RELATED WORK

Check bits are numerical methods that change message information put away in memory into code words utilizing an equipment encoder to include excess for included assurance against deficiencies. At the point when delicate flaws influence code words, causing bit flips, the check bits equipment decoder is intended to identify as well as right a predetermined number of mistakes. Check bits utilized for irregular access recollections are normally founded on direct square codes. The encoder actualizes a parallel generator lattice G and the corresponding decoder executes the equality check framework H to identify/right blunders. To encode a double message ~m, one duplicates its bit-vector by G to acquire the codeword. To unravel, one increases the put away codeword (which may have been defiled by mistakes) with the equality check lattice to acquire the disorder s, which gives blunder recognition and redress data.

Average check bits utilized for memory have the generator and equality check grids in efficient structure, i.e., the message bits are legitimately mapped into the codeword and the repetitive equality bits are affixed as far as possible of the message. This makes it simple to straightforwardly remove message information in the regular situation when no blunders happen. Check bits based methodologies can endure arbitrary piece level delicate blames yet they rapidly turned out to be ineffectual when various blunders happen because of hard blames. In the interim, incredible plans like Chip have inadmissible overheads and are not appropriate for implanted recollections. In this work, we propose novel ECC developments that have low overheads, making them appropriate for ease IoT gadgets that may encounter periodic single-piece clients.

In 1963, Wolf et al. presented error localization codes (ELC) that endeavor to recognize mistakes and distinguish the wrong fixed-length lump of the codeword. Wolf built up some key limits and concentrated how to make them utilizing the tensor result of the equality check frameworks of a mistake recognizing and a blunder remedying code. ELC has been adjusted to byte-addressable memory frameworks yet as of not long ago, they had not increased any footing in the frameworks network. As far as we could possibly know, ELCs in the routine among SED and SEC capacities has not been recently considered. We depict the essentials of Ultra-Lightweight that lie in this routine and apply explicit developments to recoup from a lion's share of single-piece delicate flaws.

## III. LITERATURE SURVEY

The system to secure the recollections used to copy the memory utilizes a for every word equality bit to distinguish single-piece blunders. At that point, when a mistake is recognized, the inherent repetition of the memory substance is utilized to attempt to address the blunder. The usage of the equality assurance. It tends to be seen that notwithstanding the match flag, a mistake flag is produced when there is a befuddle between the put away equality and the recomputed one. This is a standard equality security that can distinguish all single-piece blunders. Recognizing the blunder on each entrance is vital to stay away from off base outcomes on inquiry activities. Give us now a chance to expect that a solitary piece mistake has happened on a given word and that it is recognized with the equality check. Upon mistake identification, we can check the substance of the memory to endeavor to address the blunder. A first endeavor could be to peruse every one of the words in the memory and tally the quantity of positions that have a one for each standard. Give us a chance to signify that number as the heaviness of the standard in that memory.

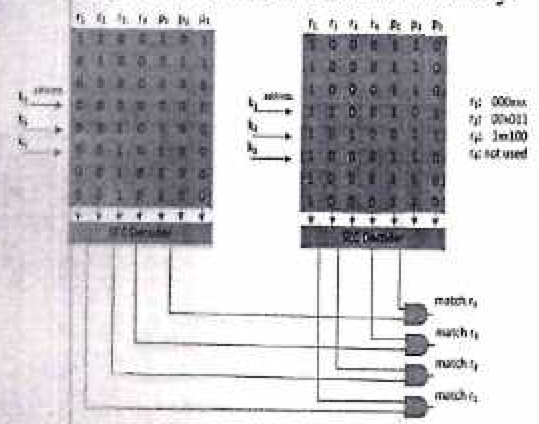

Fig. 1: EMULATION USING SRAMS

The above figure (1) shows the example how to emulate the SRAM using two cells. For instance, e3 influences r3 on the furthest left memory by changing its weight from 4 to 3. Since 3 is definitely not a substantial esteem, subsequent to distinguishing the equality blunder, we would recognize that the wrong piece is that in r3 and we would address it. This methodology would be powerful for principles that have a weight bigger than two, i.e., they have at least two "x" bits on the key bits that relate to that memory. Then again, for guidelines with a lower weight, checking the weight alone may not be sufficient. Give us now a chance to think about a standard with weight two. At that point, a blunder that changes a zero to a one will change the weight to three and the mistake will be redressed. Notwithstanding, when a one is changed to a zero (as in figure 2), at that point the new weight would be one that is a substantial esteem and the blunder can't be rectified. This, nonetheless, is less inclined to happen as just 2 positions have a one. In the event that we currently think about a weight one standard, a blunder that sets another piece to one would create a weight of two that is likewise legitimate.

Be that as it may, not all weight two blends are conceivable. This is obviously observed when taking error. All things considered, the estimations of r2 that are one would relate to key qualities 000 and 011 and those don't compare to a legitimate principle. As a rule, just positions that relate to key qualities that are at separation one from the first esteem won't be distinguished. Then again, a mistake that sets to zero the position that was one out of a weight one standard can be adjusted by checking if the standard has zero load on different recollections. In the event that that is the situation, at that point the standard is crippled and the bit isn't in mistake. Something else, the standard had a weight of one and the mistake is amended.

## IV. PRE CHARGE UNITS USING ERROR CORRECTION BITS

Content addressable memory (CAM) has been broadly utilized as a search engine that quickens the hunt of extensive look-into table. This quick hunt capacity makes CAMs alluring in the uses of system switches, processor stores, design acknowledgment, and numerous cooperative registering. The various exchanging selection lines (SLs) for the completely parallel inquiry activities come at the expense of immense unique power utilization. Here the pre charge unit is utilized to ovoid flipping when look information is steady. In the first place, so as to diminish SL control utilization, pull down ways are independently gated utilizing adaptively controlled PMOS transistors.

Since SL introduction to detach SL from ground hub isn't required, when the dismantle down ways are disengaged to SL, the SL flipping can be successfully diminished. Notwithstanding the gated SL pull down way, to decrease control utilization while improving pursuit speed, SL boosting plan is additionally embraced. By thinking about the quantity of confound and releasing velocity, the SL releasing is adaptively controlled in the proposed TCAM. At the point when the D0 and SL esteems are introduced as the put away esteem and inquiry information, individually, the SL pull down way (SL to VSS) depends on the correlation between the put away esteem and pursuit information. The below figure (2) shows the architecture of proposed system. In his pre-charge unit

PRINCIPAL/DIRECTOR
VIKAS GROUP OF INSTITUTIONS
NUNNA - 521 212
Vijayawada Rural, NTR Dist., A.P.

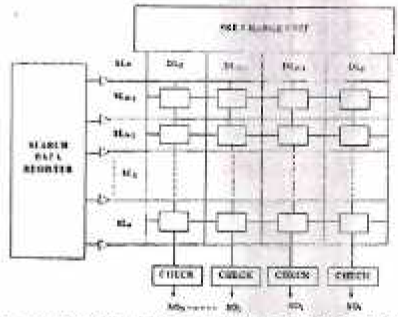

Fig. 2: PRE CHARGE UNITS USING ERROR CORRECTION BITS

D0 and SL are equivalent (coordinate), the ML pull down way is detached. In the contrary case (mismatch), they has pull down way. For the couldn't care less state, which is indicated as 'X', by putting away '1' in both D0 and D1, the draw down way is constantly detached to ML, paying little heed to the pursuit information. In view of this NOR-type TCAM cell, the ML detecting plans can be planned. If there should arise an occurrence of the pre charge-high ML detecting, the hunt activity begins with SL pre charge. , since the draw down way can be framed with initiated SL ('1'), the SL sets (SL and SLB) are introduced to '0'. the DL assessment stage, the voltage dimension of pre charge-high DL changes relying upon the examination between the put away information and pursuit information

If there should arise an occurrence of the current-sparing plan. This plan permits the SL sets to abstain from flipping when the inquiry information is consistent. Amid the DL assess stage; the present source is associated with DL, and the DL hub voltage changes relying upon the presence of draw down way. In bungle case, direct current between the present source and draw down ways builds dynamic power utilization. In spite of the fact that, the versatile current source lessens the immediate current, scattered power is as yet extensive. Here, the dL releasing pace about immerses when the quantity of bits surpasses a specific number. At the point when the quantity of confuse bits is more than 36, the ML voltage distinction diminishes perceptibly.

## V. RESULTS

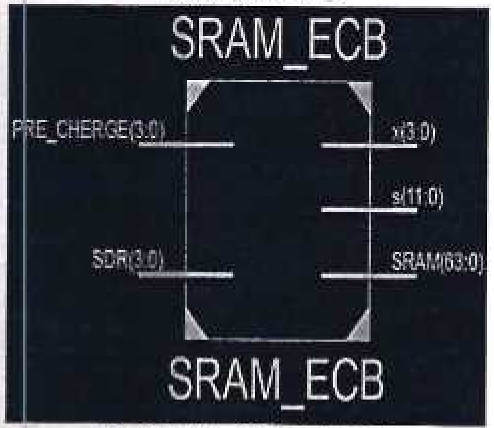


Fig. 3: RTL SCHEMATIC

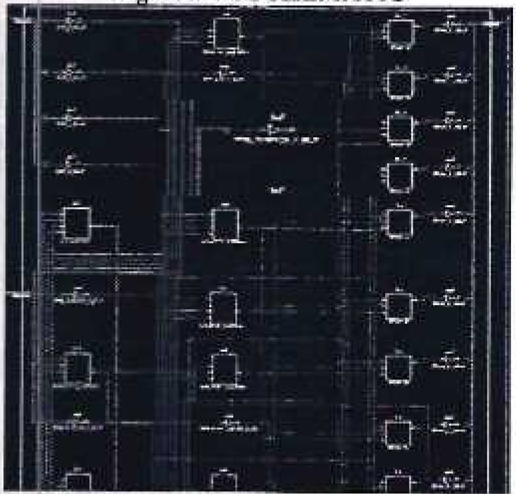

Fig. 4: TECHNOLOGY SCHEMATIC

Fig. 5: OUTPUT WAVEFORM

## VI. CONCLUSION

In this paper, to reduce the energy consumption of search operation, we design an SRAM architecture using pre charge unit, which includes the gated SL pull down paths and the SL boosting scheme. In the proposed design, the collaboratively controlled SL pull down paths facilitate the elimination of the redundant SL switching. Considering the LL discharging properties, an adaptive SL discharging scheme is also proposed to reduce SL power consumption. By applying the two-phase SL sensing, the unnecessary SL discharging can be effectively eliminated while enabling the error-free search operation. For the worst case SL, the proposed SL boosting scheme can also accelerate the search time. The simulation results show that the proposed adaptive SL discharging scheme reduces delay.

## VII. REFERENCES

[1] I. Arsovski, et al., "1.4Gsearch/s 2Mb/mm2 TCAM Using Two-PhasePrecharge ML Sensing and Power-Grid Pre-Conditioning to Reduce Ldi/dt Power-Supply Noise by 50%," IEEE Int. Solid-State Circuits Conf. (ISSCC), pp. 212-213, Feb. 2017.

[2] A. T. Do, et al., "0.77 fJ/bit/search Content Addressable Memory Using Small Match Line Swing and Automated Background Checking Scheme for Variation Tolerance," IEEE J. Solid- State Circuits, vol. 49, no. 7, pp. 1487–1498, Jul. 2014.

[3] Y. J. Chang, et al., "Low Leakage TCAM for IP Lookup Using Twoside Self-Gating," IEEE Trans. Circuits Syst. I: Reg. Papers, vol. 60, no. 6, pp. 1478-1486, June. 2013.

[4] I. Hayashi et al., "A 250-MHz 18-Mb Full Ternary CAM with LowVoltage Matchline Sensing Scheme in 65-nm CMOS," IEEE J. SolidState Circuits, vol. 48, pp. 2671–2680, Nov. 2013.

[5] S. Liu, P. Reviriego, and J. A. Maestro, "Efficient majority logic fault detection with difference-set codes for memory applications," IEEETrans. Very Large Scale Integr. (VLSI) Syst., vol. 20. no. 1, pp. 148–156, Jan. 2012.

[6] B. D. Yang, et al., "A Low Power Content Addressable Memory Using Low Swing Search Lines," IEEE Transactions on Circuits and Systems I: Regular Papers, vol. 58, no. 12, pp. 2849–2858, Dec. 2011.

[7] B. Sanghyeon, "Low-Power Ternary Content-Addressable Memory Design Using a Segmented Match Line," IEEE Trans. Circuits Syst. I: Reg. Papers, vol. 55, pp. 1485–1494, July. 2008.

[8] K. Pagiamtzis, et al., "Content-Addressable Memory (CAM) Circuits and Architectures: A Tutorial and Survey," IEEE J. Solid- State Circuits, vol. 41, pp. 712–727, Mar. 2006.

[9] E. G. Kasai et al., "200 MHz/200 MSPS 3.2W at 1.5V Vdd, 9.4Mbits Ternary CAM with New Charge Injection Match Detect Circuits and Bank Selection Scheme," in Proc. IEEE Custom Integrated Circuits Conf., CICC, 2003, pp. 387–390.

[10] D. Radaelli, H. Puchner, S. Wong, and S. Daniel, "Investigation of multi-bit upsets in a 150 nm technology SRAM device," IEEE Trans.Nucl. Sci., vol. 52, no. 6, pp. 2433–2437, Dec. 2005.

# DESIGN SRAM EMULATION WITH PRECHARGE USING ERROR CHECK BITS

[1]BATTA APARNA, [2]G. SEKHAR REDDY, [3] S KISHORE BABU
[1]M.Tech scholar, Dept of ECE, Vikas group of institutions, Nunna, Vijayawada, A.P
[2]Assistant Professor, Dept of ECE, Vikas group of institutions, Nunna, Vijayawada, A.P
[3]HOD & Associate Professor, Dept of ECE, Vikas group of institutions, Nunna, Vijayawada, A.P

**ABSTRACT: Modern ICs are enormously complicated due to decrease in device size. For high-speed memory applications such as cache, a SRAM is often used. In this paper SRAM is designed with pre charge bits using error check bits. The memories can be protected with check bits to detect errors. Single-bit errors corrected when memories are protected with check bit. by employing the gated pull down path and boosting scheme, search speed will be increased. By considering the number of mismatch and discharging speed, the discharging is adaptively controlled in the proposed system. At last the proposed system gives effective results in terms of speed and delay.**

**KEY WORDS: SRAM (static random access memory), pre charge unit, check bits, content addressable memory, error correction and location schemes.**

## I.INTRODUCTION

As CMOS innovation downsizes to nano scale and recollections are joined with an expanding number of electronic frameworks, the delicate mistake rate in memory cells is quickly expanding, particularly when recollections work in space conditions due to ionizing impacts of barometrical neutron, alpha-molecule, and enormous beams. Albeit single piece upset is a noteworthy worry about memory unwavering quality, multiple cell upsets have turned into a genuine dependability worry in some memory applications. So as to make memory cells as issue tolerant as could reasonably be expected, some error correction codes (ECCs) have been generally used to secure recollections against delicate mistakes for quite a long time. For instance, the punctured different set codes have been utilized to manage MCUs in Recollections. Yet, these codes require more area, power, and delay overheads. Since the encoding and unraveling circuits are increasingly in these confounded codes [1-2].

The general thought for accomplishing blunder location and adjustment is to include some excess (i.e., some additional information) to a message, which recipient can use to check consistency of the conveyed message, and to get information resolved to be degenerate. Mistake identification and redress plan can be either methodical or non-efficient. In a deliberate plan, the transmitter sends the interesting information, and connects a fixed number of check bits (or equality information), which are gotten from the information bits by some deterministic calculation. On the off chance that just the mistake discovery is required, a recipient would simple be able to apply a similar calculation to the got information bits and contrast its yield and the get check bits; if the qualities don't coordinate, a blunder has happened sooner or later all through the transmission [3].

Error correcting codes are normally utilized in lower-layer correspondence, As well with respect to solid stockpiling in media, for example, CDs, DVDs, hard plates and RAM. Static RAM based Field-Programmable Gate Arrays (FPGAs) are most broadly utilized in assortment of utilizations chiefly because of brief time-to market time, adaptability, high thickness, and cost-proficiency. SRAM-based FPGA stores rationale cells arrangement information in the static memory composed

PRINCIPAL/DIRECTOR
VIKAS GROUP OF INSTITUTIONS
NUNNA - 521 212
Vijayawada Rural, NTR Dist., A.P.

ISSN NO : 2249-7455

as a variety of locks. FPGA is utilized for planning complex computerized circuits. Power utilization is likewise diminished by utilizing SRAM [4]. The power utilization of SRAM differs generally relying upon how much of the time it is gotten to; it very well may be as eager for power as unique RAM, when utilized at high frequencies, and a few ICs can devour numerous watts at full data transmission. Then again, static RAM utilized at a to some degree slower pace, for example, in applications with Moderately timed microchips, draws next to no power and can have an almost unimportant power utilization when sitting inert – in the area of a couple of miniaturized.scale watts.

A few procedures have been executed to oversee control utilization of SRAM-based memory structures. FPGA gadget adjustable by SRAM comprises of a variety of programmable rationale squares interconnected by a programmable steering system and I/O squares. SRAM-based FPGA gadgets are getting to be famous in view of their elite, diminished advancement cost and re programmability. FPGAs dependent on a nanometer innovation with denser incorporation plans. Recollections are a standout amongst the most broadly utilized components in electronic frameworks. Radiation in the earth genuinely influences the usefulness of a circuit [5].

A single event upset (SEU) happens when a charged molecule, present in the earth, hits the silicon of a circuit presenting a mistake in the framework. Such mistakes in FPGA gadget influences the usefulness of the mapped plan likewise called as Soft blunders. A soft error won't harm a framework's equipment, the main harm is to the information that is being handled in the memory. To address this issue, Built-in Current Sensors (BICS) have as of late been connected related to Single Error Correction/Double Error Detection (SEC-DED) codes to shield recollections from MBUs. In any case, by utilizing those strategies no one but SEU could be revised. For both the recognition and revision of mistakes, a nonexclusive scouring plan to recreate the incorrect arrangement outline dependent on the idea of Erasure coding calculation is presented in this paper. In this sort of Erasure coding calculation, MBUs are identified by utilizing the interleaving separation which is additionally grouped into flat and vertical equality [6].

The outcomes got have demonstrated that this methodology have a lower defer overhead over different codes. built in current sensors (BICS) are actualized to help with single-blunder rectification and twofold mistake identification codes to give insurance against MBUs. Nonetheless, this strategy can just address two mistakes in a word .In this paper, the design of SRAM using error check bits is proposed. The actualized network code use calculation (number expansion and whole number subtraction) to identify blunders. Plus, the deletion codes is actualized to limit the zone overhead of additional circuits (encoder and decoder) without exasperating the entire encoding and disentangling forms.

## II. RELATED WORK

Check bits are numerical methods that change message information put away in memory into code words utilizing an equipment encoder to include excess for included assurance against deficiencies. At the point when delicate flaws influence code words, causing bit flips, the check bits equipment decoder is intended to identify as well as right a predetermined number of mistakes. Check bits utilized for irregular access recollections are normally founded on direct square codes. The encoder actualizes a parallel generator lattice G and



PRINCIPAL/DIRECTOR
VIKAS GROUP OF INSTITUTIONS
NUNNA - 521 212
Vijayawada Rural, NTR Dist., A.P.

the corresponding decoder executes the equality check framework H to identify/right blunders. To encode a double message ~m, one duplicates its bit-vector by G to acquire the codeword. To unravel, one increases the put away codeword (which may have been defiled by mistakes) with the equality check lattice to acquire the disorder s, which gives blunder recognition and redress data.

Average check bits utilized for memory have the generator and equality check grids in efficient structure, i.e., the message bits are legitimately mapped into the codeword and the repetitive equality bits are affixed as far as possible of the message. This makes it simple to straightforwardly remove message information in the regular situation when no blunders happen. Check bits based methodologies can endure arbitrary piece level delicate blames yet they rapidly turned out to be ineffectual when various blunders happen because of hard blames. In the interim, incredible plans like Chip have inadmissible overheads and are not appropriate for implanted recollections. In this work, we propose novel ECC developments that have low overheads, making them appropriate for ease IoT gadgets that may encounter periodic single-piece clients.

In 1963, Wolf et al. presented error localization codes (ELC) that endeavor to recognize mistakes and distinguish the wrong fixed-length lump of the codeword. Wolf built up some key limits and concentrated how to make them utilizing the tensor result of the equality check frameworks of a mistake recognizing and a blunder remedying code. ELC has been adjusted to byte-addressable memory frameworks yet as of not long ago, they had not increased any footing in the frameworks network. As far as we could possibly know, ELCs in the routine among SED and SEC capacities has not been recently considered. We depict the essentials of Ultra-Lightweight that lie in this routine and apply explicit developments to recoup from a lion's share of single-piece delicate flaws.

## III. LITERATURE SURVEY

The system to secure the recollections used to copy the memory utilizes a for every word equality bit to distinguish single-piece blunders. At that point, when a mistake is recognized, the inherent repetition of the memory substance is utilized to attempt to address the blunder. The usage of the equality assurance. It tends to be seen that notwithstanding the match flag, a mistake flag is produced when there is a befuddle between the put away equality and the recomputed one. This is a standard equality security that can distinguish all single-piece blunders. Recognizing the blunder on each entrance is vital to stay away from off base outcomes on inquiry activities. Give us now a chance to expect that a solitary piece mistake has happened on a given word and that it is recognized with the equality check. Upon mistake identification, we can check the substance of the memory to endeavor to address the blunder. A first endeavor could be to peruse every one of the words in the memory and tally the quantity of positions that have a one for each standard. Give us a chance to signify that number as the heaviness of the standard in that memory.

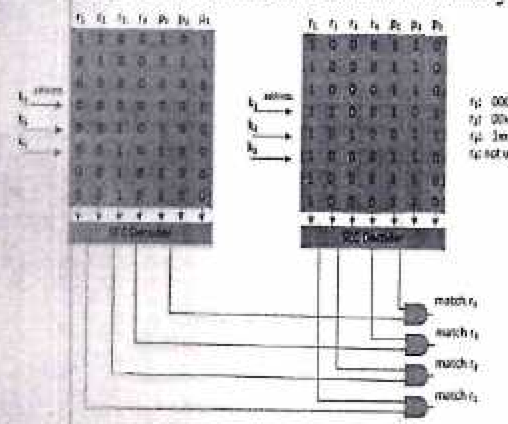

Fig. 1: EMULATION USING SRAMS



PRINCIPAL/DIRECTOR
VIKAS GROUP OF INSTITUTIONS
NUNNA - 521 212
Vijayawada Rural, NTR Dist., A.P.

The above figure (1) shows the example how to emulate the SRAM using two cells. For instance, e3 influences r3 on the furthest left memory by changing its weight from 4 to 3. Since 3 is definitely not a substantial esteem, subsequent to distinguishing the equality blunder, we would recognize that the wrong piece is that in r3 and we would address it. This methodology would be powerful for principles that have a weight bigger than two, i.e., they have at least two "x" bits on the key bits that relate to that memory. Then again, for guidelines with a lower weight, checking the weight alone may not be sufficient. Give us now a chance to think about a standard with weight two. At that point, a blunder that changes a zero to a one will change the weight to three and the mistake will be redressed. Notwithstanding, when a one is changed to a zero (as in figure 2), at that point the new weight would be one that is a substantial esteem and the blunder can't be rectified. This, nonetheless, is less inclined to happen as just 2 positions have a one. In the event that we currently think about a weight one standard, a blunder that sets another piece to one would create a weight of two that is likewise legitimate.

Be that as it may, not all weight two blends are conceivable. This is obviously observed when taking error. All things considered, the estimations of r2 that are one would relate to key qualities 000 and 011 and those don't compare to a legitimate principle. As a rule, just positions that relate to key qualities that are at separation one from the first esteem won't be distinguished. Then again, a mistake that sets to zero the position that was one out of a weight one standard can be adjusted by checking if the standard has zero load on different recollections. In the event that that is the situation, at that point the standard is crippled and the bit isn't in mistake. Something else, the standard had a weight of one and the mistake is amended.

## IV. PRE CHARGE UNITS USING ERROR CORRECTION BITS

Content addressable memory (CAM) has been broadly utilized as a search engine that quickens the hunt of extensive look-into table. This quick hunt capacity makes CAMs alluring in the uses of system switches, processor stores, design acknowledgment, and numerous cooperative registering. The various exchanging selection lines (SLs) for the completely parallel inquiry activities come at the expense of immense unique power utilization. Here the pre charge unit is utilized to ovoid flipping when look information is steady. In the first place, so as to diminish SL control utilization, pull down ways are independently gated utilizing adaptively controlled PMOS transistors.

Since SL introduction to detach SL from ground hub isn't required, when the dismantle down ways are disengaged to SL, the SL flipping can be successfully diminished. Notwithstanding the gated SL pull down way, to decrease control utilization while improving pursuit speed, SL boosting plan is additionally embraced. By thinking about the quantity of confound and releasing velocity, the SL releasing is adaptively controlled in the proposed TCAM. At the point when the D0 and SL esteems are introduced as the put away esteem and inquiry information, individually, the SL pull down way (SL to VSS) depends on the correlation between the put away esteem and pursuit information. The below figure (2) shows the architecture of proposed system. In his pre-charge unit

PRINCIPAL/DIRECTOR
VIKAS GROUP OF INSTITUTIONS
NUNNA - 521 212
Vijayawada Rural, NTR Dist., A.P.

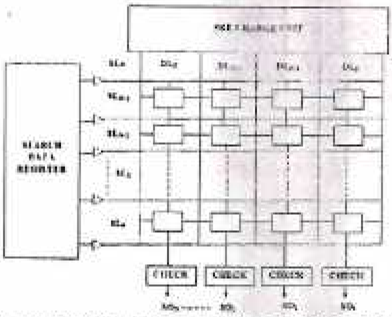

Fig. 2: PRE CHARGE UNITS USING ERROR CORRECTION BITS

D0 and SL are equivalent (coordinate), the ML pull down way is detached. In the contrary case (mismatch), they has pull down way. For the couldn't care less state, which is indicated as 'X', by putting away '1' in both D0 and D1, the draw down way is constantly detached to ML, paying little heed to the pursuit information. In view of this NOR-type TCAM cell, the ML detecting plans can be planned. If there should arise an occurrence of the pre charge-high ML detecting, the hunt activity begins with SL pre charge. , since the draw down way can be framed with initiated SL ('1'), the SL sets (SL and SLB) are introduced to '0'. the DL assessment stage, the voltage dimension of pre charge-high DL changes relying upon the examination between the put away information and pursuit information

If there should arise an occurrence of the current-sparing plan. This plan permits the SL sets to abstain from flipping when the inquiry information is consistent. Amid the DL assess stage; the present source is associated with DL, and the DL hub voltage changes relying upon the presence of draw down way. In bungle case, direct current between the present source and draw down ways builds dynamic power utilization. In spite of the fact that, the versatile current source lessens the immediate current, scattered power is as yet extensive. Here, the dL releasing pace about immerses when the quantity of bits surpasses a specific number. At the point when the quantity of confuse bits is more than 36, the ML voltage distinction diminishes perceptibly.

## V. RESULTS

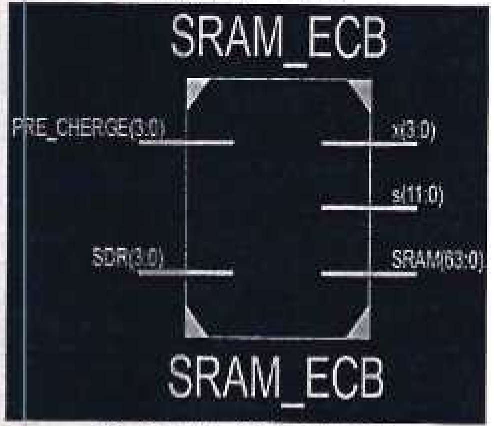


Fig. 3: RTL SCHEMATIC

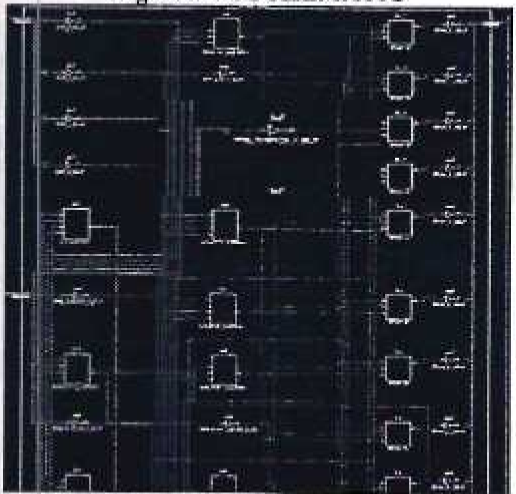

Fig. 4: TECHNOLOGY SCHEMATIC

Fig. 5: OUTPUT WAVEFORM

## VI. CONCLUSION

In this paper, to reduce the energy consumption of search operation, we design an SRAM architecture using pre charge unit, which includes the gated SL pull down paths and the SL boosting scheme. In the proposed design, the collaboratively controlled SL pull down paths facilitate the elimination of the redundant SL switching. Considering the LL discharging properties, an adaptive SL discharging scheme is also proposed to reduce SL power consumption. By applying the two-phase SL sensing, the unnecessary SL discharging can be effectively eliminated while enabling the error-free search operation. For the worst case SL, the proposed SL boosting scheme can also accelerate the search time. The simulation results show that the proposed adaptive SL discharging scheme reduces delay.

## VII. REFERENCES

[1] I. Arsovski, et al., "1.4Gsearch/s 2Mb/mm2 TCAM Using Two-PhasePrecharge ML Sensing and Power-Grid Pre-Conditioning to Reduce Ldi/dt Power-Supply Noise by 50%," IEEE Int. Solid-State Circuits Conf. (ISSCC), pp. 212-213, Feb. 2017.

[2] A. T. Do, et al., "0.77 fJ/bit/search Content Addressable Memory Using Small Match Line Swing and Automated Background Checking Scheme for Variation Tolerance," IEEE J. Solid- State Circuits, vol. 49, no. 7, pp. 1487–1498, Jul. 2014.

[3] Y. J. Chang, et al., "Low Leakage TCAM for IP Lookup Using Twoside Self-Gating," IEEE Trans. Circuits Syst. I: Reg. Papers, vol. 60, no. 6, pp. 1478-1486, June. 2013.

[4] I. Hayashi et al., "A 250-MHz 18-Mb Full Ternary CAM with LowVoltage Matchline Sensing Scheme in 65-nm CMOS," IEEE J. SolidState Circuits, vol. 48, pp. 2671–2680, Nov. 2013.

[5] S. Liu, P. Reviriego, and J. A. Maestro, "Efficient majority logic fault detection with difference-set codes for memory applications," IEEETrans. Very Large Scale Integr. (VLSI) Syst., vol. 20, no. 1, pp. 148–156, Jan. 2012.

[6] B. D. Yang, et al., "A Low Power Content Addressable Memory Using Low Swing Search Lines," IEEE Transactions on Circuits and Systems I: Regular Papers, vol. 58, no. 12, pp. 2849–2858, Dec. 2011.

[7] B. Sanghyeon, "Low-Power Ternary Content-Addressable Memory Design Using a Segmented Match Line," IEEE Trans. Circuits Syst. I: Reg. Papers, vol. 55, pp. 1485–1494, July. 2008.

[8] K. Pagiamtzis, et al., "Content-Addressable Memory (CAM) Circuits and Architectures: A Tutorial and Survey," IEEE J. Solid- State Circuits, vol. 41, pp. 712–727, Mar. 2006.

[9] E. G. Kasai et al., "200 MHz/200 MSPS 3.2W at 1.5V Vdd, 9.4Mbits Ternary CAM with New Charge Injection Match Detect Circuits and Bank Selection Scheme," in Proc. IEEE Custom Integrated Circuits Conf., CICC, 2003, pp. 387–390.

[10] D. Radaelli, H. Puchner, S. Wong, and S. Daniel, "Investigation of multi-bit upsets in a 150 nm technology SRAM device," IEEE Trans.Nucl. Sci., vol. 52, no. 6, pp. 2433–2437, Dec. 2005.